GEOPHYSICAL RESEARCH LETTERS, VOL. 17, NO. 9, PAGES 1433-1436, AUGUST 1990

TOMOGRAPHIC P-WAVE VELOCITY IMAGES OF THE LOMA PRIETA EARTHQUAKE ASPERITY

Jonathan M. Lees[1]

Department of Geology and Geophysics, Yale University

Abstract. Tomographic inversion is applied to delay times from local earthquakes to image 3-D velocity variations surrounding the main rupture of the 1989 Loma Prieta earthquake. The 55x45 square km region is represented by blocks of 1 km per side laterally and by 8 layers of varying thickness to 18 km depth. High quality P-wave arrival times recorded on the USGS CALNET array from 549 crustal earthquakes with depths of 0 to 25 km were used as sources. Preliminary results several velocity variations (5-12%) that correlate with specific characteristics of the 1989 rupture. These include prominent high-velocity anomalies near the mainshock hypocenter and prominent low-velocity anomalies where the dip of the San Andreas fault appears to change significantly. The termination of prominent low velocity features existing primarily in the hanging wall to depths of 7-9 km, correlates with the top of the rupture zone. High-velocity variations along the fault dominate where aftershock activity is high. The high velocity anomaly located at depth along the fault is interpreted as imaging the asperity on which the Loma Prieta earthquake occurred.

Introduction

The structural features of the San Andreas fault in the Loma Prieta region are complicated by reverse and strike-slip faulting subparallel to the San Andreas, including left, or restraining, steps along these faults [Aydin and Page, 1984]. The southwestern Salinian block (Figure 1) is characterized by granitic plutons overlain by Eocene and Oligocene shales. To the northeast, the Franciscan complex includes Cretaceous melanges and serpentinites. Seismic refraction profiles near the southeastern portion of the target area indicated a low velocity (3.34 km/s) zone spanning the San Andreas fault, between the Sargent and the Zayante-Vergeles faults, which was interpreted as evidence for low grade metamorphism of local sediments [Mooney and Colburn, 1985; Bakun and McLaren, 1984]. Northeast of the Sargent fault, velocities appear to be considerably higher (4.5 km/s). The deformation associated with the recent Loma Prieta earthquake indicates that significant oblique-reverse faulting extends to depths of 20 km [Lisowski et al., 1990].

Data Selection

The data used in this study was selected from the USGS catalogue of 5000 events recorded in the month of October, 1989. Events with fewer than 8 station readings, rms residuals

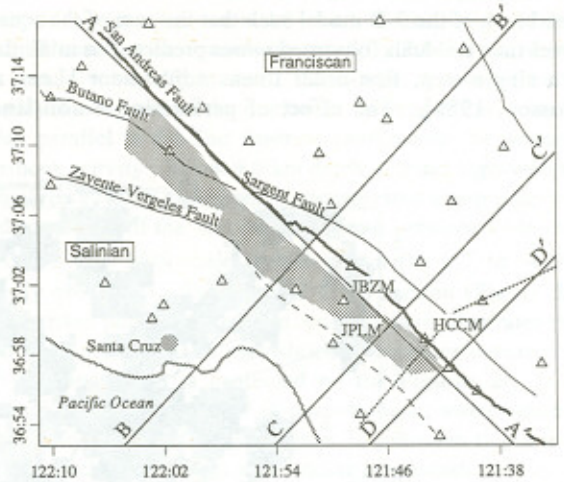

Fig. 1: Map of target area and station distribution (triangles) of the USGS seismic network. Major faults, such as the San Andreas Fault, Sargent Fault, Butano Fault are indicated. Cross sections AA', BB', CC', DD' for Figure 3 are indicated for reference as are three stations mentioned in the text. The stippled area represents approximate rupture zone based on seismicity plots. The dashed line between cross section DD' and CC' is the location of the refraction study by Mooney and Colburn [1985].

> 0.3, horizontal errors > 2.5 km and vertical errors > 5.0 km were excluded as well as observations made by automatic (RTP) picking, observations given a low weight(4) and raypaths to stations outside of the target volume. All the travel data used were made by USGS observers. From the remaining high quality hypocenters, 549 earthquakes were located within the target region, producing 6683 raypaths. Two 1-D models, separated by the San Andreas fault (Table 1; D. Oppenhiemer, personal communication, USGS), were used to determine initial calculated travel times. Travel-time residuals were determined by taking the difference between observed and predicted travel-times through the 1-D models, less a station correction (supplied by the USGS), to remove the effect of near receiver structure.

Table 1. One-Dimensional reference velocity models

Depth (km)	Franciscan (km/s)	Salinian (km/s)
0.0	3.34	3.42
0.5	4.23	4.35
1.0	5.01	4.58
3.0	5.63	5.10
5.0	5.89	5.59
7.0	6.24	6.06
9.0	6.26	6.23
13.0	6.30	6.24
18.0	6.69	6.64
25.0	8.00	8.00

[1] Formerly at Institute for Crustal Studies, University of California, Santa Barbara.

Paper number 90GL01495
0094-8276/90/90GL-01495$03.00

Methodology

The target volume was divided into a 55×45 grid region using 1.0 km-square blocks of varying thickness following the 1-D reference velocity models, resulting in a maximum of 24,000 model parameters. Rays were traced through the 1-D models and perturbations of slowness were calculated within each block of the 3-D model such that the sum of the squared travel-time residuals (observed minus predicted) is minimized, in a single step, first-order linear adjustment [Lees and Crosson, 1989]. The effect of performing a non-linear inversion by using the 3-D model to re-locate the earthquakes and update the raypaths is the subject of current investigations and is beyond the scope of this paper. However, since the anomalies observed in this study are typically less than 10%, I expect the effect of hypocenter relocation to be relatively small. The data were weighted according to estimates of the original quality factors (0-3) provided with each phase reading. Effects of noisy data were reduced by constraining the Laplacian (second spatial derivative) of the slowness field to be small within horizontal layers, effectively smoothing the model laterally. The resulting system of simultaneous equations was

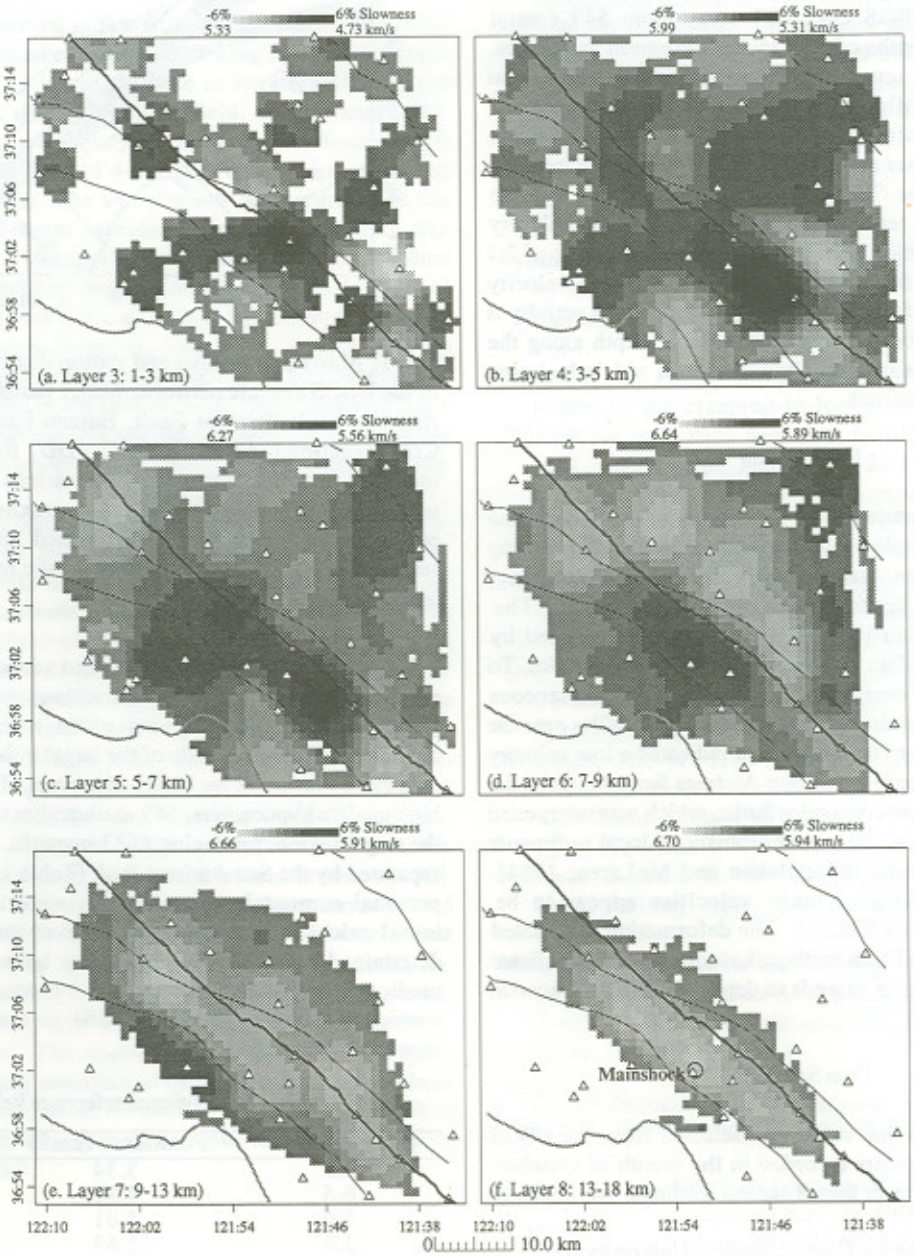

Fig. 2a-f: Tomographic inversion for Loma Prieta, CA. Horizontal cross sections partitioned according to the 1-D reference velocity model (Table 1). Dark areas represent zones zones of low velocity perturbations (high slowness) and light shades represent high velocity anomalies (low slowness). Results are plotted as percent perturbation from two 1-D reference velocity models on each side of the San Andreas Fault, with a common scale from -6.0 to 6.0% with corresponding velocity indicated. The actual scales for each layer may differ from these scale limits. Blocks not penetrated by any rays are white.

solved by an iterative conjugate gradient technique [Lees and Crosson, 1989] and the sum of squared travel time residuals was reduced to 34% of its initial value.

The influence of data variability on the model, was estimated by Jackknife error analysis [Lees and Crosson, 1989]. The standard errors (1 σ) calculated in this manner were found to be typically 1% or less (slowness perturbation) over most of the model, suggesting slowness variations greater than a few percent are significant. Resolution was estimated by calculating impulse responses for different parts of the model [Lees and Crosson, 1989]. Near the center of the model, where the ray coverage is most dense, the lateral resolution length was found to be slightly better than 4 km (3-4 blocks). The resolution kernels, however, are typically not symmetric, due to heterogeneity of ray coverage.

Results

The inversion results are displayed as grayshade plots for layers 3-8 (Figure 2a-f) and four cross sections (Figure 3a-d). By displaying perturbations from the two 1-D models, the regional velocity structures, which would otherwise dominate the image, are removed. The top two layers of the model (0.0-1.0 km depth) have poor lateral resolution because the emerging, near-vertical rays are concentrated near the receiving stations. The perturbations range from -1 to +1% anomaly and are viewed as additions to the station corrections removed prior to inversion. Between 3.0-7.0 km depth there is a low velocity anomaly between 36°58'-37°02' latitude north at 121°46' longitude west (between stations JBZM, HCCM and JPLM, Figures 1 and 2) which apparently spans the surface trace of the San Andreas fault. This feature exhibits a slowness anomaly of ~9.0% (the display in Figure 2b is clipped at 6%), corresponding to velocities of 4.71 km/s for the Salinian Block and 5.13 km/s on the Franciscan side. By 7.0-9.0 km depth, this anomaly has diminished. Similarly, a low velocity anomaly is observed to the northwest forming a low-velocity wedge parallel to the San Andreas fault above the primary aftershock activity. Below 9.0 km depth, a broad high-velocity anomaly is evident and appears concentrated along a narrow band southwest of the San Andreas Fault between 13.0-18.0 km depth (the ±6% scale is wider than the 0.7 to -4.0% actually observed). The vertical cross section (Figure 3a) which strikes parallel to the San Andreas fault illustrates this trend quite clearly. The mainshock hypocenter occurred at 16.5 km depth and is projected on the Figures 2f, 3a-c. Although the vast majority of aftershocks occur within zones of higher velocity perturbation, Figure 3a indicates that a high velocity patch immediately surrounding the mainshock has less seismicity. The seismicity shown in figures 3c and 3d suggest that the San Andreas fault apparently changes dip (from ~67° to ~76°) along strike, southeast of station HCCM (Figure 1).

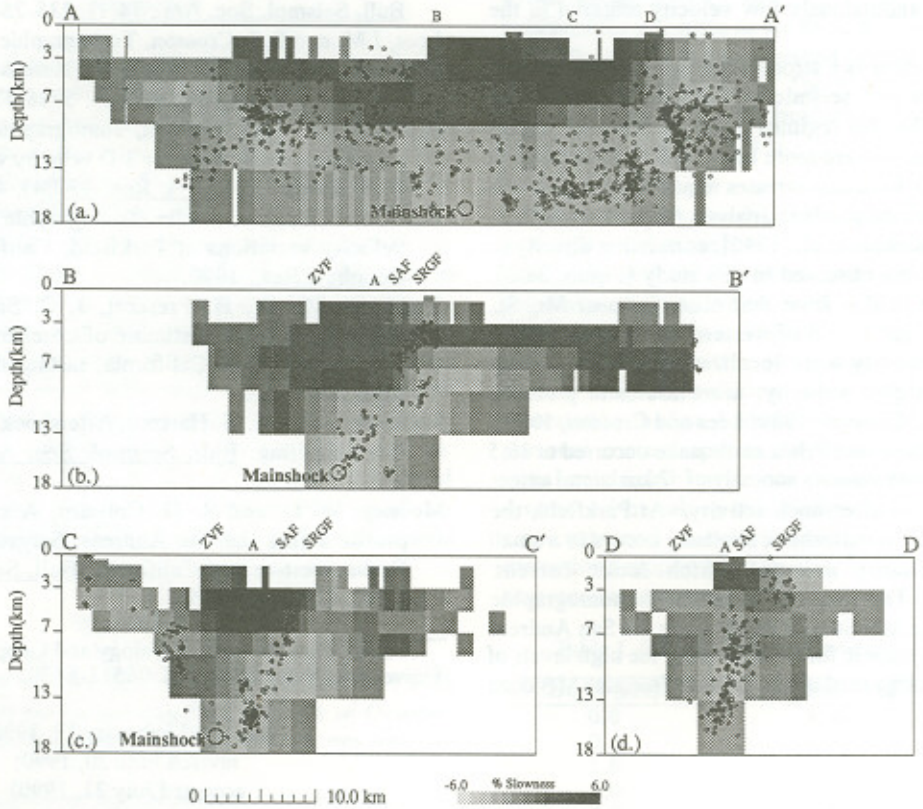

Fig. 3a-d: Cross section AA' running parallel to the San Andreas fault along the zone of highest seismicity. Sections BB', CC', DD' are perpendicular to the San Andreas bisecting it near cross section AA'. Each section is marked where it geographically intersects the others as are the major faults, with SAF=San Andreas Fault, ZVF=Zayante-Vergeles Fault, SRGF=Sargent Fault. Earthquakes are projected horizontally from a swath 4 km wide centered on the cross section mapped in Figure 1. Notice the correlation of the seismicity to the higher velocity regions.

Discussion

The prominent low-velocity anomaly between 1.0-7.0 km depth extending 7-10 km along the San Andreas fault between the Sargent and the Zayante-Vergeles faults (including the one between stations JBZM, HCCM and JPLM) is consistent with previous observations of a low seismic velocities in this area by Mooney and Colburn [1985]. They observed a 3.34-5.45 km/s (~35%) velocity contrast at 2.5 km depth where as I observe a ~9.0% anomaly extending to 5-7 km depth (Figure 3c). The higher velocity anomalies observed northeast of the Sargent fault (Figure 2a-d) also agree with the model of Mooney and Colburn [1985], as well as with observations made by Bakun and Mclaren [1984].

Anomalies observed in this study using aftershocks of the Loma Prieta earthquake bear some striking resemblances to a similar 3-D velocity inversion done at Parkfield, California [Lees and Malin, 1990]. At Parkfield, a high-amplitude (>10%), low-velocity anomaly spanning the San Andreas fault and extending to a depth of 4-5 km, is observed southeast of the 1966 mainshock. The velocity low is interpreted as the result of local basement subsidence produced by strike-slip deformation around changes in local fault geometry. At Loma Prieta, the corresponding anomaly occurs above the location of where the San Andreas fault, as defined by seismicity, appears to change dip (Figures 3c and d). The nearly 10° change of dip within a few kilometers along strike of the fault suggests a major bend, or warp, in the fault at depth. Such a feature could produce extensional opening near the surface northwest of the bend and result in anomalously low velocity material in the same region.

In both studies there is a strong correlation between high-velocity anomalies and seismicity, suggesting that major earthquakes in strike-slip regimes occur in zones of higher velocity, where materials are more brittle and more competent and thus more likely to sustain stresses required for high levels of seismicity. Based on geodetic analysis the fault extends 6-18 km in depth [Lisowski et al., 1990], correlating directly to the high velocity zone observed in this study (Figure 3a-c). This characteristic differs from that observed near Mt. St. Helens or in the Puget Sound of western Washington where zones of high seismicity were localized in lower velocity regions between higher velocity, more aseismic plutonic intrusions [Lees and Crosson, 1989; Lees and Crosson, 1990]. The mainshock of the Loma Prieta earthquake occurred at 16.5 km depth within a high velocity anomaly of ~7 km lateral extent exhibiting little or no aftershock activity. At Parkfield, the hypocenter of the 1966 mainshock similarly occurs in a small patch of high-velocity material which lacks current microearthquakes. The implication is that the tomographic inversion is imaging asperities at depth along the San Andreas fault which are responsible for concentrating the high levels of stress that produce large earthquake ruptures [see also Mendoza and Hartzell, 1988].

Conclusion

Tomographic images along the San Andreas fault near the Loma Prieta earthquake indicate low-velocity anomalies southwest of the fault to depths of 7-9 km where an apparent transition zone exists. Below this depth predominantly higher velocity anomalies are observed to correlate with the region of intense seismicity to a depth of 18 km. These are interpreted as being brittle, competent materials associated with the asperities of the fault. A prominent low-velocity feature is observed near the southeastern end of the Loma Prieta rupture where the San Andreas fault apparently changes dip.

Acknowledgements. The author acknowledges and is grateful for the useful suggestions and comments of C. Nicholson, P. Malin, M. Alvarez and anonymous reviewers in preparing this manuscript. The Seismology Branch of the USGS, Menlo Park, provided the data for this study. UCSB contribution number 0045-06EQ-10CS.

References

Aydin, A., and B.M. Page, Diverse Pliocene-Quaternary tectonics in a transform environment, San Francisco Bay region, California, Geol. Soc. Am. Bull. 95, 1303-1317, 1984.

Bakun, W. H., and M. McLaren, Micro earthquakes and the nature of the creeping-to-locked transition of the San Andreas fault zone near San Juan Bautista, California, Bull. Seismol. Soc. Am., 74(1), 235-254, 1984.

Lees, J.M. and R.S. Crosson, Tomographic inversion for 3-D velocity structure at Mount St. Helens using earthquake data, J. Geophys. Res., 94(B5), 5716-5728, 1989.

Lees, J.M., and R.S. Crosson, Tomographic imaging of local earthquake delay times for 3-D velocity variation in western Washington,J.Geophys. Res., 95(B4), 4763-4776, 1990.

Lees, J. M., and P. E. Malin, Tomographic images of P-wave velocity variations at Parkfield, California, in press J. Geophys. Res., 1990.

Lisowski, M., W. H. Prescott, J. C. Savage, and M. J. Johnson, Geodetic estimate of coseismic slip during the 1989 Loma Prieta, California, earthquake, Geophys. Res. Lett., this issue.

Mendoza, C. and S. H. Hartzell, Aftershock patterns and main shock faulting, Bull. Seismol. Soc. Am., 78(4), 1438-1449, 1988.

Mooney, W. D. and R. H. Colburn, A seismic-refraction profile across the San Andreas, Sargent, and Calaveras Faults, west-central California, Bull. Seismol. Soc. Am., 75(1), 175-191, 1985.

J. Lees, Department of Geology and Geophysics, Yale University, New Haven, CT 06511-8130.

(Received February 19, 1990;
revised June 20, 1990;
accepted July 21, 1990)